

Resonant tunneling through a quantum dot weakly coupled to quantum wires or quantum Hall edge states

A. Furusaki

Yukawa Institute for Theoretical Physics, Kyoto University, Kyoto 606-8502, Japan

(Received 16 July 1997)

Resonant tunneling through a quantum dot weakly coupled to Tomonaga-Luttinger liquids is discussed. The linear conductance due to sequential tunneling is calculated by solving a master equation for temperatures below and above the average level spacing in the dot. When the parameter g characterizing the Tomonaga-Luttinger liquid is smaller than $1/2$, the resonant tunneling process is incoherent down to zero temperature. At low temperature T the height and width of the conductance peaks in the Coulomb blockade oscillations are proportional to $T^{1/g-2}$ and T , respectively. The contribution from tunneling via a virtual intermediate state (cotunneling) is also included. The resulting conductance formula can be applied for the resonant tunneling between edge states of fractional quantum Hall liquids with filling factor $\nu = 1/(2m + 1) = g$. [S0163-1829(98)01212-0]

I. INTRODUCTION

Advances in nanostructure technology have made it possible to fabricate semiconductor devices such as quantum dots,¹ small two-dimensional regions in which electrons are confined. The transport properties of the quantum dots weakly coupled via tunnel barriers to external leads have recently attracted much attention. At low temperatures the linear conductance exhibits periodic peak structures as a function of a gate voltage, a phenomenon known as Coulomb blockade oscillations. These peaks occur when the energy change due to tunneling of one electron into or out of the dot equals the Fermi energy of the leads. Apart from these resonance points, tunneling is suppressed due to the Coulomb blockade.^{2,3} Single-particle energy levels in a small quantum dot are discrete with mean level spacing Δ and have decay width $\Gamma_{L(R)}$ which is proportional to the tunneling rate to the left (right) lead. In the temperature regime $\Gamma_{L(R)} \ll T \ll \Delta$, the line shape of the conductance peaks is⁴

$$G = \frac{e^2}{\hbar} \frac{\Gamma_L \Gamma_R}{\Gamma_L + \Gamma_R} \left(-\frac{d}{d\varepsilon} \right) \frac{1}{e^{\varepsilon/T} + 1}, \quad (1)$$

where ε is proportional to the gate voltage measured relative to the resonance point. Equation (1) is valid when the external leads are Fermi liquids and has been used to interpret numerous experimental data.

In this paper we discuss a generalization of Eq. (1) to the case where the external leads are Tomonaga-Luttinger (TL) liquids. The TL liquids can be realized in very narrow quantum wires⁵ or as edge states of fractional quantum Hall liquids.⁶⁻⁸ Figure 1 shows schematic pictures of the systems of our interest, a quantum dot coupled via tunnel barriers to one-dimensional (1D) quantum wires or to edge states in fractional quantum Hall liquids. In both cases it is assumed that there are small but finite matrix elements for the tunneling from the points B and C of the zero-dimensional states formed in the quantum dot to the points A and D of the 1D TL liquids. To fully understand the transport in these sys-

tems, it is necessary to take into account both the charging energy and the discrete energy levels in the dot.

This paper is intended to give a simplified description of the resonant tunneling between TL liquids. We extend the theory of the sequential tunneling developed in Refs. 9 and 10 to derive a generalized formula of the linear conductance, and discuss the validity of the sequential-tunneling picture. Instead of applying the instanton technique starting from an effective action for bosonic variables,⁹ we use a master-equation approach to calculate the resonant current through a quantum dot.¹¹ This method is more direct and transparent, and has been successful in describing the Coulomb blockade oscillations in quantum dots coupled to Fermi-liquid leads.^{4,12} With this method we can describe in a unified way the resonant tunneling through a quantum dot which is weakly coupled to TL-liquid reservoirs as well as to ordinary Fermi-liquid reservoirs. We will see that our formula has even the same form as the conductance of double quantum dots weakly coupled to Fermi-liquid reservoirs.¹³ Another

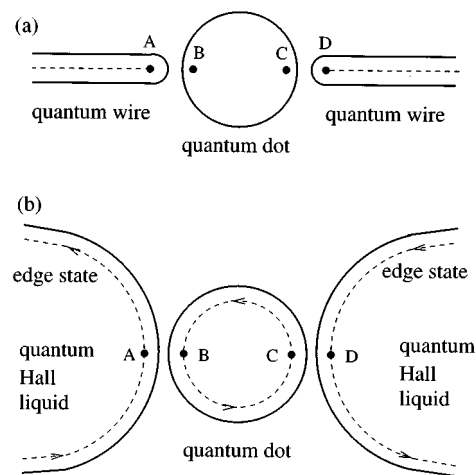


FIG. 1. Quantum dot coupled to (a) quantum wires and (b) edge states in quantum Hall liquids. Dotted lines represent one-dimensional states.

merit of this approach is that it allows us to easily treat a system with two TL-liquid reservoirs having different interaction parameters. This situation corresponds to, for example, the resonant tunneling from a $\nu=1/3$ edge state to a $\nu=1$ edge state.

The use of the master-equation approach can be justified because the resonant current is mainly carried by sequential tunneling processes down to zero temperature when the interaction parameter g characterizing TL liquids is smaller than $1/2$.⁹ When $g \geq 1/2$, on the other hand, there is a crossover temperature below which the transport becomes coherent and the line shape of the peak conductance approaches the universal form obtained by Kane and Fisher.¹⁴ For the edge states in the fractional quantum Hall liquid with a filling factor $\nu=1/(2m+1)$, the parameter g equals ν .⁶ This means that the tunneling between edge states via a quantum dot can be described, down to zero temperature, by the sequential-tunneling picture discussed in this paper, unless the bare tunneling elements are large and/or $\nu=1$. Finally we note that our approach is different from the previous work by Kinaret *et al.*¹⁵ in which the edge states in the quantum dot are described as chiral TL liquids but the leads are assumed to be Fermi liquids. In our study, on the other hand, the leads are described as TL liquids and the states in the dot are treated as 0D states. Thus we are interested in the effects coming from anomalous power-law correlations in the TL leads.

II. MODEL

In this section we introduce a simple model for a dot and leads, and calculate propagators in the leads. The Hamiltonian of the system shown in Fig. 1 can be separated into four parts, $H=H_L+H_R+H_D+H_T$, with $H_{L(R)}$ describing the left (right) lead, H_D the dot, and H_T the tunneling between the leads and the dot. Since the tunneling rate through the tunnel barriers is assumed to be very small, the number of electrons in the dot is a good quantum number. Thus we may write the dot Hamiltonian

$$H_D = \sum_N \sum_{i=0}^{\infty} E(N,i) |N,i\rangle \langle N,i|, \quad (2)$$

where N is the number of electrons in the dot and $E(N,i)$ is eigenenergy of the many-body state $|N,i\rangle$ [$E(N,0) < E(N,1) < E(N,2) < \dots$]. In this paper we will not try to calculate the energies $E(N,i)$ themselves, but instead we assume that they are given, since we are mainly interested in the line shape of conductance peaks in the Coulomb blockade oscillations, not in the position of these peaks. Without loss of generality, we may assume that $E(N_0,0)$ and $E(N_0+1,0)$ are the two lowest energies among $E(N,i=0)$'s. The energy differences $E(N_0-1,0) - E(N_0,0)$ and $E(N_0+2,0) - E(N_0+1,0)$ are of the order of the charging energy E_C . A convenient choice to represent this would be the approximation usually made in studies of the Coulomb blockade² $E(N,0) = (E_C/2)(N - \mathcal{N})^2$, where \mathcal{N} ($N_0 < \mathcal{N} < N_0+1$) is an external parameter which can be controlled by changing the gate voltage. Since we are interested in the temperature range $T \ll E_C$, we neglect the states in which $N \neq N_0, N_0+1$. Then the current flow is accompanied by the periodic change of

the electron numbers,¹² $N_0 \rightarrow N_0+1 \rightarrow N_0 \rightarrow \dots$. We also note that the ratio Δ/E_C can be much smaller than 1 for both systems shown in Fig. 1.^{16,17}

First we address the situation shown in Fig. 1(a). The left (L) and right (R) leads are described as TL liquids whose interaction parameter is $K_{\rho L(R)}$ for the charge sector and $K_{\sigma L(R)}$ for the spin sector.¹⁸ Due to repulsive electron-electron interactions K_{ρ} is less than 1 while K_{σ} is fixed at 1 because of the SU(2) spin symmetry. In the bosonized form H_L is written as

$$H_L = \hbar \int_0^{\infty} dk (v_{cL} k a_{k,L}^{\dagger} a_{k,L} + v_{sL} k b_{k,L}^{\dagger} b_{k,L}), \quad (3)$$

where $a_{k,L}$ ($b_{k,L}$) is an annihilation operator of bosons describing charge (spin) density fluctuations propagating with velocity $v_{c(s)L}$. The Hamiltonian of the right lead H_R can be written in a similar way. The tunneling Hamiltonian is given by

$$H_T = t_L \sum_{\sigma} [\psi_{\sigma}^{\dagger}(A) \psi_{\sigma}(B) + \psi_{\sigma}^{\dagger}(B) \psi_{\sigma}(A)] \\ + t_R \sum_{\sigma} [\psi_{\sigma}^{\dagger}(C) \psi_{\sigma}(D) + \psi_{\sigma}^{\dagger}(D) \psi_{\sigma}(C)], \quad (4)$$

where $\psi_{\sigma}(X)$ annihilates an electron with spin up ($\sigma=+1$) or down ($\sigma=-1$) at the point X ($X=A, B, C$, and D in Fig. 1). The electron field operator at the boundary may be written as¹⁹

$$\psi_{\sigma}(A) = \sqrt{\frac{2}{\pi\alpha}} \exp \left[\int_0^{\infty} dk \frac{e^{-\alpha k/2}}{\sqrt{2K_{\rho L} k}} (a_{k,L} - a_{k,L}^{\dagger}) \right. \\ \left. + \sigma \int_0^{\infty} dk \frac{e^{-\alpha k/2}}{\sqrt{2k}} (b_{k,L} - b_{k,L}^{\dagger}) \right], \quad (5)$$

where α is a short-distance cutoff of the order of the reciprocal of the Fermi wave number k_F . This leads to local propagators

$$\langle \psi_{\sigma}^{\dagger}(A,t) \psi_{\sigma}(A,0) \rangle_L = \langle \psi_{\sigma}(A,t) \psi_{\sigma}^{\dagger}(A,0) \rangle_L \\ = \frac{c_A}{\alpha} \left\{ \frac{i\Lambda}{\pi T} \sinh \left[\frac{\pi T(t-i\delta)}{\hbar} \right] \right\}^{-1/g_L}, \quad (6)$$

where c_A is a dimensionless constant of order 1, Λ is a high-energy cutoff or a band width, δ is positive infinitesimal, and $g_L^{-1} = \frac{1}{2}(1/K_{\rho L} + 1)$. The thermal averages are calculated with respect to H_L , and $\psi_{\sigma}(A,t) = \exp(iH_L t/\hbar) \psi_{\sigma}(A) \exp(-iH_L t/\hbar)$. Similarly, the propagators at the point D are obtained as

$$\langle \psi_{\sigma}^{\dagger}(D,t) \psi_{\sigma}(D,0) \rangle_R = \langle \psi_{\sigma}(D,t) \psi_{\sigma}^{\dagger}(D,0) \rangle_R \\ = \frac{c_D}{\alpha} \left\{ \frac{i\Lambda}{\pi T} \sinh \left[\frac{\pi T(t-i\delta)}{\hbar} \right] \right\}^{-1/g_R}, \quad (7)$$

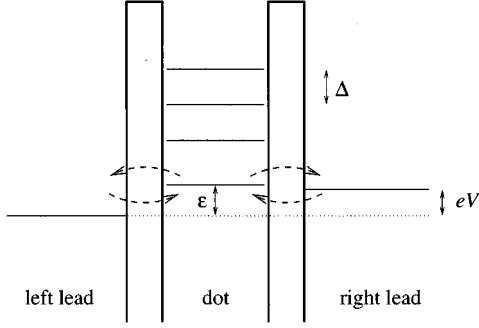


FIG. 2. Schematic picture of energy diagrams. Horizontal lines in the leads represent Fermi levels. There are four tunneling processes.

where c_D is a dimensionless constant, $g_R^{-1} = \frac{1}{2}(1/K_{\rho R} + 1)$ and the averages are taken with respect to H_R . Note that g_L and g_R are smaller than 1 because both $K_{\rho L}$ and $K_{\rho R}$ are smaller than 1.

Although we have considered the system shown in Fig. 1(a), both Eqs. (6) and (7) also hold for the quantum Hall edge states in Fig. 1(b). Suppose that the left lead and the right lead are in the quantum Hall regime with filling factors $\nu_L = 1/(2l+1)$ and $\nu_R = 1/(2m+1)$ (l, m : integers), respectively.²⁰ In this case the Hamiltonian for the left edge states is

$$H_L = \frac{v}{4\pi} \int dx \left(\frac{d\varphi(x)}{dx} \right)^2, \quad (8)$$

where x is the coordinate along the edge and the bosonic field $\varphi(x)$ obeys $[\varphi(x), \varphi(y)] = i\pi \text{sgn}(x-y)$.⁶ Since the electron field operator at the point A is given by $\psi(A, t) \propto \exp[i\varphi(A, t)/\sqrt{\nu_L}]$,^{6,21} we find the correlation function in the left edge is also given by Eq. (6) with $g_L = \nu_L$. The same derivation also holds for the right edge: $g_R = \nu_R$. In the following sections, we shall use the parameters g_L and g_R without distinguishing the two systems. Since the electron spin is not important in the following discussion, we will suppress the spin indices in the electron field operator.

III. LOW-TEMPERATURE REGIME ($\Gamma \ll T < \Delta$)

In this section we calculate the linear conductance for $T \leq \Delta$ within the master-equation approach.¹² In this approach we assume that the energy is conserved in each tunneling process, and neglect the contributions from tunneling via virtual intermediate states. We will see later that this assumption is valid near the conductance peaks in the weak-tunneling limit. In the following calculation we include only low-energy states $|N, i\rangle$ with $N = N_0$ or $N_0 + 1$ which are major contributors in the conduction process at temperature $T \leq \Delta \ll E_C$, a situation often satisfied in experiments using semiconductor quantum dots.^{22,23} A schematic energy diagram is shown in Fig. 2.

In lowest order in H_T the transition rates from the state $|N_0, i\rangle$ to the state $|N_0 + 1, j\rangle$ due to the tunneling of an electron into the dot through the left or right tunnel barrier are calculated from the golden rule:

$$P_L(N_0, i; N_0 + 1, j) = \left(\frac{t_L}{\hbar} \right)^2 \int_{-\infty}^{\infty} dt e^{-i\varepsilon_{ij}t/\hbar} \times | \langle N_0 + 1, j | \psi^\dagger(B) | N_0, i \rangle |^2 \times \langle \psi^\dagger(A, t) \psi(A, 0) \rangle_L, \quad (9a)$$

$$P_R(N_0, i; N_0 + 1, j) = \left(\frac{t_R}{\hbar} \right)^2 \int_{-\infty}^{\infty} dt e^{-i(\varepsilon_{ij} - eV)t/\hbar} \times | \langle N_0 + 1, j | \psi^\dagger(C) | N_0, i \rangle |^2 \times \langle \psi^\dagger(D, t) \psi(D, 0) \rangle_R, \quad (9b)$$

where $\varepsilon_{ij} = E(N_0 + 1, j) - E(N_0, i)$ and eV is the difference between the chemical potentials of the left and the right leads. The transition rates for the inverse processes are similarly given by

$$P_L(N_0 + 1, j; N_0, i) = \left(\frac{t_L}{\hbar} \right)^2 \int_{-\infty}^{\infty} dt e^{i\varepsilon_{ij}t/\hbar} \times | \langle N_0, i | \psi(B) | N_0 + 1, j \rangle |^2 \times \langle \psi(A, t) \psi^\dagger(A, 0) \rangle_L, \quad (9c)$$

$$P_R(N_0 + 1, j; N_0, i) = \left(\frac{t_R}{\hbar} \right)^2 \int_{-\infty}^{\infty} dt e^{i(\varepsilon_{ij} - eV)t/\hbar} \times | \langle N_0, i | \psi(C) | N_0 + 1, j \rangle |^2 \times \langle \psi(D, t) \psi^\dagger(D, 0) \rangle_R. \quad (9d)$$

Using the propagators (6) and (7), we evaluate the integrals (9a)–(9d),

$$P_L(N_0, i; N_0 + 1, j) = \frac{T}{\hbar} e^{-\varepsilon_{ij}2T} \gamma_L(N_0, i; N_0 + 1, j), \quad (10a)$$

$$P_R(N_0, i; N_0 + 1, j) = \frac{T}{\hbar} e^{-(\varepsilon_{ij} - eV)2T} \gamma_R(N_0, i; N_0 + 1, j), \quad (10b)$$

$$P_L(N_0 + 1, j; N_0, i) = \frac{T}{\hbar} e^{\varepsilon_{ij}2T} \gamma_L(N_0, i; N_0 + 1, j), \quad (10c)$$

$$P_R(N_0 + 1, j; N_0, i) = \frac{T}{\hbar} e^{(\varepsilon_{ij} - eV)2T} \gamma_R(N_0, i; N_0 + 1, j), \quad (10d)$$

where $\gamma_L(N_0, i; N_0 + 1, j)$ and $\gamma_R(N_0, i; N_0 + 1, j)$ are expressed using the Γ function as

$$\gamma_L(N_0, i; N_0 + 1, j) = \frac{\Gamma_{Lij} \left(\frac{\pi T}{\Lambda} \right)^{1/g_L - 1}}{2\pi T} \times \frac{|\Gamma(1/2g_L + i(\varepsilon_{ij}/2\pi T))|^2}{\Gamma(1/g_L)}, \quad (11a)$$

$$\gamma_R(N_0, i; N_0 + 1, j) = \frac{\Gamma_{Rij} \left(\frac{\pi T}{\Lambda} \right)^{1/g_R - 1}}{2\pi T} \times \frac{|\Gamma(1/2g_R + i(\varepsilon_{ij} - eV/2\pi T))|^2}{\Gamma(1/g_R)}. \quad (11b)$$

We have defined $\Gamma_{Lij} = (2\pi c_A t_L^2 / \alpha \Lambda) |\langle N_0, i | \psi(B) | N_0 + 1, j \rangle|^2$ and $\Gamma_{Rij} = (2\pi c_D t_R^2 / \alpha \Lambda) |\langle N_0, i | \psi(C) | N_0 + 1, j \rangle|^2$. The time evolution of $P(N_0, i)$, the probability that the state $|N_0, i\rangle$ is occupied, obeys the master equation

$$\begin{aligned} \frac{\partial}{\partial t} P(N_0, i) = \sum_j \{ & P(N_0 + 1, j) [P_L(N_0 + 1, j; N_0, i) + P_R(N_0 \\ & + 1, j; N_0, i)] - P(N_0, i) [P_L(N_0, i; N_0 + 1, j) \\ & + P_R(N_0, i; N_0 + 1, j)] \}. \end{aligned} \quad (12)$$

In the steady state where $(\partial/\partial t)P(N_0, i) = 0$, we need to solve a set of detailed balance relations

$$\begin{aligned} P(N_0, i) [P_L(N_0, i; N_0 + 1, j) + P_R(N_0, i; N_0 + 1, j)] \\ = P(N_0 + 1, j) [P_L(N_0 + 1, j; N_0, i) + P_R(N_0 + 1, j; N_0, i)]. \end{aligned} \quad (13)$$

In equilibrium where $V = 0$, $P(N_0, i)$ is given by

$$P_{\text{eq}}(N_0, i) = \frac{\exp[-E(N_0, i)/T]}{\sum_{N_0} \sum_i \exp[-E(N_0, i)/T]}, \quad (14)$$

so that from Eqs. (10a)–(10d) we can easily see that Eq. (13) is satisfied. Following Ref. 4, we solve Eq. (13) to the first order in V . We first substitute $P(N_0, i) = P_{\text{eq}}(N_0, i) [1 + (eV/T)p(N_0, i)]$ into Eq. (13) and linearize it with respect to V . We find

$$\begin{aligned} p(N_0 + 1, j) - p(N_0, i) \\ = \frac{\gamma_R(N_0, i; N_0 + 1, j)}{\gamma_L(N_0, i; N_0 + 1, j) + \gamma_R(N_0, i; N_0 + 1, j)}. \end{aligned} \quad (15)$$

The current through the quantum dot is then given, up to first order in V , by

$$\begin{aligned} I = -e \sum_{i,j} [& P(N_0, i) P_L(N_0, i; N_0 + 1, j) \\ & - P(N_0 + 1, j) P_L(N_0 + 1, j; N_0, i)] \\ = \frac{e^2 V}{\hbar} \sum_{i,j} e^{-\varepsilon_{ij}/2T} P_{\text{eq}}(N_0, i) & \gamma_L(N_0, i; N_0 + 1, j) \\ \times [p(N_0 + 1, j) - p(N_0, i)] & \end{aligned} \quad (16)$$

from which we get the linear conductance

$$\begin{aligned} G = \frac{e^2}{\hbar} \sum_{i,j} e^{-\varepsilon_{ij}/2T} P_{\text{eq}}(N_0, i) \\ \times \frac{\gamma_L(N_0, i; N_0 + 1, j) \gamma_R(N_0, i; N_0 + 1, j)}{\gamma_L(N_0, i; N_0 + 1, j) + \gamma_R(N_0, i; N_0 + 1, j)}, \end{aligned} \quad (17)$$

which is a generalization of Eq. (3.14) of Ref. 4.

For the rest of this section, let us concentrate on the temperature regime $T \ll \Delta$. In this regime we may assume that the dot is always in the lowest energy state with a given electron number, so that we may set $i = j = 0$ in Eq. (17). We can thus write $P_{\text{eq}}(N_0, 0)$ as

$$P_{\text{eq}}(N_0, 0) = \frac{1}{1 + e^{-\varepsilon/T}}, \quad (18)$$

where $\varepsilon = E(N_0 + 1, 0) - E(N_0, 0)$. From Eqs. (17) and (18) we find the linear conductance²⁴ for $T \ll \Delta$

$$G = \frac{e^2}{2\hbar \cosh(\varepsilon/2T)} \frac{\gamma_L(\varepsilon, T) \gamma_R(\varepsilon, T)}{\gamma_L(\varepsilon, T) + \gamma_R(\varepsilon, T)}, \quad (19)$$

where $\gamma_{L,R}(\varepsilon, T) = \gamma_{L,R}(N_0, 0; N_0 + 1, 0)$. This is the generalization of Eq. (1) to the case where the leads are TL liquids. When $g_{L(R)}^{-1}$ is an integer, $\gamma_{L(R)}(\varepsilon, T)$ has a simple expression. For example,

$$\gamma_L(\varepsilon, T) = \begin{cases} \frac{\Gamma_L}{2T \cosh(\varepsilon/2T)}, & g_L = 1 \\ \frac{\varepsilon \Gamma_L}{4\Lambda T \sinh(\varepsilon/2T)}, & g_L = \frac{1}{2} \\ \frac{\Gamma_L(\pi^2 T^2 + \varepsilon^2)}{16\Lambda^2 T \cosh(\varepsilon/2T)}, & g_L = \frac{1}{3}, \end{cases} \quad (20)$$

where we have used the simplified notation $\Gamma_L = \Gamma_{L00}$. Thus, Eq. (19) reduces to Eq. (1) when $g_L = g_R = 1$. It is interesting to observe that when $g_L = g_R = 1/2$ Eq. (19) reduces to

$$G = \frac{e^2}{4\hbar \Lambda} \frac{\Gamma_L \Gamma_R}{\Gamma_L + \Gamma_R} \frac{\varepsilon/T}{\sinh(\varepsilon/T)}, \quad (21)$$

which has the same ε and T dependence as the conductance of a quantum dot coupled to Fermi-liquid leads ($g = 1$) at $\Delta \ll T \ll E_C$ obtained by Glazman and Shekhter.¹² This coincidence occurred because of the effective halving of g in this temperature regime,⁹ which we will discuss in the next section. It is also interesting to see that Matveev *et al.*¹³ have derived a formula similar to Eq. (19) for the conductance of double quantum dots, although the parameter g has completely different physical meaning in their case. Figure 3 shows the line shape of the linear conductance Eq. (19) for the symmetric case $\Gamma_L = \Gamma_R$ and $g_L = g_R = 1, 1/2$, and $1/3$. The conductance is normalized by the peak conductance of the $g = 1$ case, $G_{\text{max}} = e^2 \Gamma / 8\hbar T$. For fixed Γ and ε , G becomes smaller with decreasing g . If scaled properly, however, the three curves in Fig. 3 can be made very similar to each other. This is because for any g the width of the peaks is proportional to T and the conductance decays exponentially for large $|\varepsilon|$. For example, the conductance of the $g = 1/2$ case (21) is almost proportional to that of the $g = 1$ case (1) with $T \rightarrow 1.25T$.⁴ It is the temperature dependence of the peak conductance, $G(\varepsilon = 0) \propto T^{1/g-2}$, that differs qualitatively. We hope this can be tested experimentally in the near future. The anomalous temperature dependence of the peak

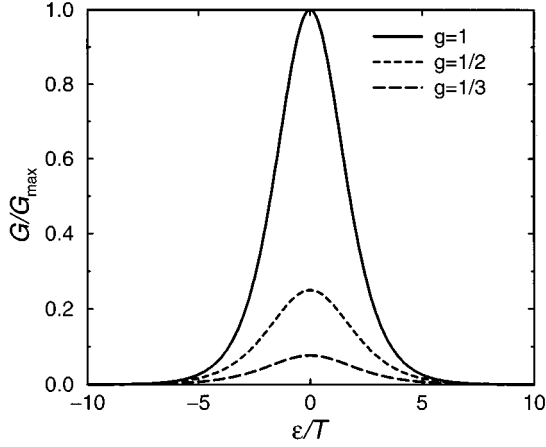


FIG. 3. The linear conductance due to the sequential tunneling Eq. (19) for $g_L = g_R = g = 1, 1/2$, and $1/3$. The conductance is normalized by the peak value of the $g = 1$ case $G_{\max} = e^2 \Gamma / 8 \hbar T$. We have set $T/\Lambda = 0.25$.

conductance is a signature of the power-law decay of the propagators in the TL liquids, Eqs. (6) and (7).

When the left and right leads are different TL liquids ($g_L \neq g_R$), the peak conductance is roughly given by $\{\max[T/\Gamma_L(T/\Lambda)^{1-1/g_L}, T/\Gamma_R(T/\Lambda)^{1-1/g_R}]\}^{-1}$. If $g_L < 1/2$ and $g_R > 1/2$, and $\gamma_R(0, T) \ll \gamma_L(0, T) \ll 1$ at some temperature ($T < \Delta$), then the conductance may have a nonmonotonic temperature dependence. With lowering temperature, the peak conductance first increases as $G \propto T^{1/g_R - 2}$ and then decreases as $G \propto T^{1/g_L - 2}$. This nonmonotonic temperature dependence would be observed, for example, for the sequential tunneling between the $\nu = 1$ edge state and the $\nu = 1/3$ edge state. When both g_L and g_R are larger (smaller) than $1/2$, on the other hand, the conductance should monotonically increase (decrease) with decreasing temperature.

Next we examine when the sequential-tunneling approximation is valid for temperatures $T \ll \Delta$. We find two conditions to be satisfied. First, the conductance calculated perturbatively in the tunneling matrix elements must be much smaller than the conductance quantum e^2/h . This leads to the condition $\gamma_L(0, T) \ll 1$ and $\gamma_R(0, T) \ll 1$, or equivalently,

$$T \ll \Lambda \left(\frac{\Lambda}{\Gamma_{L,R}} \right)^{g_{L,R}/(1-2g_{L,R})} \quad (22)$$

when $g_{L,R} < 1/2$ and

$$T \gg \Lambda \left(\frac{\Gamma_{L,R}}{\Lambda} \right)^{g_{L,R}/(2g_{L,R}-1)} \quad (23)$$

when $g_{L,R} > 1/2$. For the Fermi-liquid leads ($g = 1$) this condition reduces to $T \gg \Gamma$. Note that, when $g < 1/2$, the condition (22) is satisfied down to zero temperature, once it is valid at some high temperature. Second, the current carried by virtual tunneling processes must be negligibly small compared with the contribution from the sequential tunneling processes we have calculated. For $\varepsilon \gg T$ the second-order perturbation in H_T yields the operator for the virtual tunneling

$$H_{\text{vt}} = \frac{t_L t_R}{\varepsilon} [\psi^\dagger(A) \psi(B) \psi^\dagger(C) \psi(D) + \text{H.c.}] \quad (24)$$

In lowest order, the probability that an electron virtually tunnels from the left lead to the right lead is

$$P_{\text{vt}}(L \rightarrow R) = \left(\frac{t_L t_R}{\hbar \varepsilon} \right)^2 \int_{-\infty}^{\infty} dt e^{-ieVt/\hbar} \langle \psi^\dagger(A, t) \psi(A, 0) \rangle_L \\ \times \langle \psi(B, t) \psi^\dagger(C, t) \psi^\dagger(B, 0) \psi(C, 0) \rangle_D \\ \times \langle \psi(D, t) \psi^\dagger(D, 0) \rangle_R. \quad (25)$$

We may neglect the time-dependence of the two-particle propagator in the dot for $T \ll \Delta$, and write $\langle \psi^\dagger(B, t) \psi(C, t) \psi(B, 0) \psi^\dagger(C, 0) \rangle_D = c_2$. Here c_2 is a constant which may depend on the geometry and the mean free path of the dot.²⁵ From Eqs. (6), (7), and (25), we get

$$P_{\text{vt}}(L \rightarrow R) = \frac{c_3 \Gamma_L \Gamma_R \Lambda}{4 \pi^2 \hbar \varepsilon^2} e^{-eV/2T} \left(\frac{\pi T}{\Lambda} \right)^{1/g_L + 1/g_R - 1} \\ \times \frac{|\Gamma(1/2g_L + 1/2g_R + i(eV/2\pi T))|^2}{\Gamma(1/g_L + 1/g_R)}, \quad (26)$$

where c_3 is a dimensionless constant. The probability of the reverse process is $P_{\text{vt}}(R \rightarrow L) = e^{eV/T} P_{\text{vt}}(L \rightarrow R)$. Hence the linear conductance due to the virtual tunneling is

$$G_{\text{vt}} = \lim_{V \rightarrow 0} \frac{-e}{V} [P_{\text{vt}}(L \rightarrow R) - P_{\text{vt}}(R \rightarrow L)] \\ = \frac{c_3 e^2 \Gamma_L \Gamma_R}{4 \pi \hbar \varepsilon^2} \frac{|\Gamma(1/2g_L + 1/2g_R)|^2}{\Gamma(1/g_L + 1/g_R)} \left(\frac{\pi T}{\Lambda} \right)^{1/g_L + 1/g_R - 2}. \quad (27)$$

This contribution has the same temperature dependence $T^{1/g_L + 1/g_R - 2}$ as that of the tunneling between TL liquids coupled by a single tunnel barrier.¹⁴ In the case of Fermi-liquid leads ($g_L = g_R = 1$), G_{vt} is independent of temperature, and the virtual tunneling process contributing to G_{vt} is called the elastic cotunneling.²⁵ When $\varepsilon \leq T$, the temperature T serves as a lower cutoff so that ε^2 in the denominator of the right-hand side of Eq. (27) should be replaced with $(|\varepsilon| + 2\pi T)^2$. When $|\varepsilon| \ll T$, the conductance G , Eq. (19), is much larger than G_{vt} if Eq. (22) or (23) is satisfied. On the other hand, using the relation $|\Gamma[1/2g + i(\varepsilon/2\pi T)]|^2 \approx 2\pi(\varepsilon/2\pi T)^{1/g-1} e^{-\varepsilon/2T}$ for $\varepsilon \gg T$, we find that the condition for $G \gg G_{\text{vt}}$ at $\varepsilon \gg T$ is equivalent to

$$\frac{e^{-\varepsilon/T}}{T} \left[\frac{1}{\Gamma_L} \left(\frac{\varepsilon}{\Lambda} \right)^{1-1/g_L} + \frac{1}{\Gamma_R} \left(\frac{\varepsilon}{\Lambda} \right)^{1-1/g_R} \right]^{-1} \\ \gg \frac{\Gamma_L \Gamma_R}{\varepsilon^2} \left(\frac{\pi T}{\Lambda} \right)^{1/g_L + 1/g_R - 2}. \quad (28)$$

For $g_L = g_R = g$ this condition is simplified to

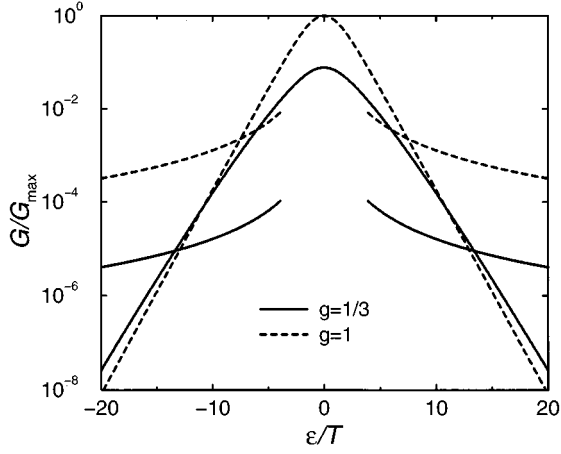


FIG. 4. Line shape of a conductance peak. Both the contribution from the sequential tunneling Eq. (19) and that of the virtual tunneling process Eq. (27) are shown for $g_L = g_R = g = 1$ and $1/3$. The conductance is normalized by the peak value of the $g = 1$ case $G_{\max} = e^2 \Gamma / 8 \hbar T$. We have set $T/\Lambda = 0.25$, $\Gamma/T = 0.2$, and $c_3 = 1$.

$$\varepsilon \lesssim T \ln \left[\frac{T}{\Gamma_{L,R}} \left(\frac{\Lambda}{T} \right)^{1/g-1} \right], \quad (29)$$

in which the argument of logarithm is much larger than 1 if the condition $\gamma_{L,R}(0, T) \ll 1$ is satisfied.

From these considerations we conclude that, when Eq. (22) or (23) is satisfied, the line shape of conductance peaks is described by Eq. (19) around a peak and by Eq. (27) away from the peak, see Fig. 4.

Finally we briefly comment on the Kondo effect in the resonant tunneling through a very small quantum dot or an impurity level. In the Fermi-liquid case ($g_L = g_R = 1$) it has been shown^{26,27} using the Anderson model that the conductance due to tunneling processes via a virtual intermediate state logarithmically increases with lowering temperature and eventually approaches $2e^2/h$ in the zero-temperature limit. In the TL-liquid case ($g_L, g_R < 1$) this kind of Kondo effect does not happen for $|\varepsilon| \gtrsim T$, because $G_{\text{vt}} \propto T^{1/g_L + 1/g_R - 2}$. In other words the virtual tunneling is irrelevant in the renormalization-group sense, in contrast to the Fermi-liquid case where the virtual tunneling is marginally relevant. Nevertheless there exists an analog of the Kondo effect in the TL liquid case when $g_L = g_R = 1/2$. In this case, as we saw in Eq. (21), the peak conductance $G(\varepsilon = 0)$ is independent of temperature in the lowest-order calculation. In fact, one can show^{14,28} that on resonance ($\varepsilon = 0$) the tunneling is marginally relevant so that the peak conductance increases logarithmically with lowering temperature when higher-order terms are included. It is, however, important to note that our problem is not exactly the same as the (multi-channel) Kondo effect due to the interference between the tunneling processes through the left and right barriers, unlike the situation ($\Delta \ll T \ll E_C$) discussed by Matveev.²⁸

IV. HIGH-TEMPERATURE REGIME ($\Delta \ll T \ll E_C$)

Let us next consider the high-temperature case where $\Delta \ll T \ll E_C$. We note that, although we can only expect $\Delta \lesssim E_C$ in general, the condition $\Delta \ll E_C$ can be satisfied in some relatively large quantum dots. In this temperature re-

gime we may still assume that the number of electrons in the dot is either N_0 or $N_0 + 1$. However, the electrons in the dot no longer stay in the lowest-energy state but occupy excited states. This gives time dependence to the propagators in the dot. At $T \gg \Delta$ we can regard the discrete energy levels as continuum,¹² and the propagators in the dot may be written as

$$\begin{aligned} \langle \psi^\dagger(\mathbf{B}, t) \psi(\mathbf{B}, 0) \rangle_D &= \langle \psi(\mathbf{B}, t) \psi^\dagger(\mathbf{B}, 0) \rangle_D \\ &= \rho_B \left\{ \frac{i\Delta}{\pi T} \sinh \left[\frac{\pi T(t - i\delta)}{\hbar} \right] \right\}^{-1/g_D}, \end{aligned} \quad (30a)$$

$$\begin{aligned} \langle \psi^\dagger(\mathbf{C}, t) \psi(\mathbf{C}, 0) \rangle_D &= \langle \psi(\mathbf{C}, t) \psi^\dagger(\mathbf{C}, 0) \rangle_D \\ &= \rho_C \left\{ \frac{i\Delta}{\pi T} \sinh \left[\frac{\pi T(t - i\delta)}{\hbar} \right] \right\}^{-1/g_D}, \end{aligned} \quad (30b)$$

where ρ_B and ρ_C are electron densities at the point B and C. Without a magnetic field [Fig. 1(a)] the exponent g_D is 1 (Fermi liquid), whereas g_D equals the filling factor $\nu_D = 1/(2n + 1)$ if the dot is in the fractional quantum Hall regime [Fig. 1(b)]. Using Eqs. (6), (7), (30a), and (30b), we can repeat the calculation in the previous section to derive the linear conductance in the sequential tunneling approximation. Since the excited states are already taken into account in Eqs. (30a) and (30b), we can simply use the result for the single-level case ($T \ll \Delta$), Eq. (19), with appropriate modification. We thus find that the conductance is given by

$$G = \frac{e^2}{2\hbar \cosh(\varepsilon/2T)} \frac{\tilde{\gamma}_L(\varepsilon, T) \tilde{\gamma}_R(\varepsilon, T)}{\tilde{\gamma}_L(\varepsilon, T) + \tilde{\gamma}_R(\varepsilon, T)} \quad (31)$$

with

$$\begin{aligned} \tilde{\gamma}_{L(R)}(\varepsilon, T) &= \frac{\tilde{\Gamma}_{L(R)}}{2\pi T} \left(\frac{\pi T}{\Lambda} \right)^{1/g_{L(R)} - 1} \left(\frac{\pi T}{\Delta} \right)^{1/g_D} \\ &\quad \times \frac{|\Gamma(1/2g_{L(R)} + 1/2g_D + i(\varepsilon/2\pi T))|^2}{\Gamma(1/g_{L(R)} + 1/g_D)}. \end{aligned} \quad (32)$$

Here $\tilde{\Gamma}_L = 2\pi c_A t_L^2 \rho_B / \alpha \Lambda$ and $\tilde{\Gamma}_R = 2\pi c_D t_R^2 \rho_C / \alpha \Lambda$. The parameters g_L and g_R are effectively changed into $g_L \rightarrow \tilde{g}_L \equiv g_L g_D / (g_L + g_D)$ and $g_R \rightarrow \tilde{g}_R \equiv g_R g_D / (g_R + g_D)$. Note that, when $g_{L(R)} = g_D$, the parameter $g_{L(R)}$ is effectively halved:⁹ $\tilde{g}_{L(R)} = g_{L(R)} / 2$. This is the reason why Eq. (19) with $g_L = g_R = 1/2$ reproduced the high-temperature conductance of a quantum dot coupled to Fermi-liquid leads ($g_L = g_R = 1$).¹²

The same exponent $\tilde{g}_{L(R)}$ also appears in the conductance due to the virtual tunneling process. This virtual tunneling is known as the inelastic cotunneling in the Fermi-liquid case.²⁵ For $T \gg \Delta$ an electron tunneling through the left tunnel barrier may be different from an electron tunneling through the right barrier, so that we may approximate the two-

particle propagator as $\langle \psi(B,t)\psi^\dagger(C,t)\psi^\dagger(B,0)\psi(C,0) \rangle_D \approx \langle \psi(B,t)\psi^\dagger(B,0) \rangle_D \langle \psi^\dagger(C,t)\psi(C,0) \rangle_D$. From Eqs. (6), (7), (25), (30a), and (30b), we get

$$G_{\text{vt}} = \frac{e^2 \bar{\Gamma}_L \bar{\Gamma}_R}{8 \pi \hbar \varepsilon} \frac{|\Gamma(1/2g_L + 1/2g_R + 1/g_D)|^2}{\Gamma(1/g_L + 1/g_R + 2/g_D)} \times \left(\frac{\pi T}{\Lambda} \right)^{1/g_L + 1/g_R - 2} \left(\frac{\pi T}{\Delta} \right)^{2/g_D}. \quad (33)$$

The conductance is proportional to $T^{1/g_L + 1/g_R + 2/g_D - 2}$. For the Fermi-liquid case ($g_L = g_R = g_D = 1$) this reduces to $G_{\text{vt}} \propto T^2$, in agreement with the inelastic cotunneling theory.²⁵

V. CONCLUSIONS

In this paper we have studied the resonant tunneling through a quantum dot coupled to TL liquids in the weak-tunneling limit. We have considered both the sequential tunneling process and the tunneling process via a virtual intermediate state (cotunneling) to calculate the linear conductance at temperatures $T \ll E_C$. Within this approximation we have determined the line shape of the conductance peaks as a function of a gate voltage. At $T \leq \Delta$ the peak height and width are proportional to $T^{1/g-2}$ and T , respectively. This approach is justified in the weak-tunneling limit where the conductance is much smaller than e^2/h . In contrast to the Fermi-liquid case ($g=1$) where the approximation breaks down at $T < \Gamma$, our result [Eqs. (19) and (27)] is valid down to zero temperature when the TL-liquid parameters g_L and g_R are smaller than 1/2.

The edge states of the fractional quantum Hall liquids with filling factor $\nu = 1/(2m+1)$ correspond to the case $g = \nu$. Hence the tunneling through a quantum dot weakly coupled to the edge states is described by our theory in the whole temperature range. We hope that the theory can be tested experimentally in the near future. The anomalous temperature dependence of the peak height $T^{1/\nu-2}$ and careful fitting of the line shape to Eq. (19) will give another firm

evidence for the TL-liquid behavior of the edge states. The anomalous exponent $1/\nu-2$ is a direct consequence of the power-law tunnel density of states $\rho(E) \propto E^{1/\nu-1}$ in TL leads and of the discrete energy spectrum $\rho(E) \propto \delta(E)$ in a quantum dot. It is also interesting to note that, when a quantum dot is weakly coupled to the $\nu=1$ edge at one tunneling contact and to the $\nu=1/3$ edge states at the other, the linear conductance may exhibit a nonmonotonic temperature dependence.

We note that there are some cases in which the sequential-tunneling picture is not applicable even when the bare tunneling matrix elements are small. For example, if g_L and g_R are larger 1/2, the tunneling rates through the left and right tunnel barrier grow with decreasing temperature. This means that the transport through a quantum dot becomes coherent and the sequential-tunneling approximation breaks down at low temperature where $\gamma(0,T) \geq 1$. This coherent transport in the low-temperature limit is described better starting from the small-barrier (strong-tunneling) limit. In this limit it was shown by Kane and Fisher¹⁴ that in the symmetric case ($g_L = g_R > 1/2$ and $t_L = t_R$) the backward scattering is renormalized to zero when $\varepsilon = 0$ and that the line shape of conductance peaks approaches a universal form^{14,29-31} below a crossover temperature at which $\gamma(0,T) \approx 1$. This is also the case for systems with $g_L = g_R = 1/2$, in which the tunneling at $\varepsilon = 0$ is marginally relevant¹⁴ and increases logarithmically with decreasing temperature.²⁸ We emphasize again, however, that for the resonant tunneling between the edge states in the fractional quantum Hall liquids as well as between the 1D quantum wires with sufficiently strong repulsive interactions, the sequential-tunneling approach developed in this paper gives the correct description even in the low-temperature limit.

ACKNOWLEDGMENTS

The author would like to thank A. MacDonald and N. Nagaosa for useful discussions and M. Sigrist for helpful comments on the manuscript.

- ¹M. A. Kastner, Rev. Mod. Phys. **64**, 849 (1992), and references therein.
- ²D. V. Averin and K. K. Likharev, in *Mesoscopic Phenomena in Solids*, edited by B. L. Altshuler, P. A. Lee, and R. A. Webb (North-Holland, Amsterdam, 1991).
- ³*Single Charge Tunneling*, edited by H. Grabert and M. H. Devoret (Plenum, New York, 1992).
- ⁴C. W. J. Beenakker, Phys. Rev. B **44**, 1646 (1991).
- ⁵S. Tarucha, T. Honda, and T. Saku, Solid State Commun. **94**, 413 (1995).
- ⁶X. G. Wen, Int. J. Mod. Phys. B **6**, 1711 (1992).
- ⁷F. P. Milliken, C. P. Umbach, and R. A. Webb, Solid State Commun. **97**, 309 (1996).
- ⁸A. M. Chang, L. N. Pfeiffer, and K. W. West, Phys. Rev. Lett. **77**, 2538 (1996).
- ⁹A. Furusaki and N. Nagaosa, Phys. Rev. B **47**, 3827 (1993).
- ¹⁰C. de C. Chamon and X. G. Wen, Phys. Rev. Lett. **70**, 2605 (1993).

- ¹¹Chamon and Wen (Ref. 10) used a method which is equivalent to the master-equation approach to calculate the current through a single impurity level. In this sense the present paper can be viewed as a generalization of Ref. 10 to the case where there are many impurity levels.
- ¹²L. I. Glazman and R. I. Shekhter, J. Phys.: Condens. Matter **1**, 5811 (1989); I. O. Kulik and R. I. Shekhter, Sov. Phys. JETP **41**, 308 (1975).
- ¹³K. A. Matveev, L. I. Glazman, and H. U. Baranger, Phys. Rev. B **54**, 5637 (1996).
- ¹⁴C. L. Kane and M. P. A. Fisher, Phys. Rev. B **46**, 15 233 (1992).
- ¹⁵J. M. Kinaret, Y. Meir, N. S. Wingreen, P. A. Lee, and X.-G. Wen, Phys. Rev. B **46**, 4681 (1992).
- ¹⁶A. Furusaki and K. A. Matveev, Phys. Rev. Lett. **75**, 709 (1995); Phys. Rev. B **52**, 16 676 (1995).
- ¹⁷H. Yi and C. L. Kane, Phys. Rev. B **53**, 12 956 (1996).
- ¹⁸See, for example, H. J. Schulz, in *Mesoscopic Quantum Physics*, Les Houches Session LXI, edited by E. Akkermans *et al.* (Elsevier, Amsterdam, 1995).

- ¹⁹S. Eggert and I. Affleck, Phys. Rev. B **46**, 10 866 (1992); A. Furusaki and N. Nagaosa, Phys. Rev. Lett. **72**, 892 (1994); M. Fabrizio and A. O. Gogolin, Phys. Rev. B **51**, 17 827 (1995); S. Eggert, H. Johannesson, and A. Mattsson, Phys. Rev. Lett. **76**, 1505 (1996).
- ²⁰In these quantum Hall states the electrons are spin polarized, so that we can neglect spin indices.
- ²¹The particles tunneling between the quantum dot and a quantum Hall edge state are electrons, not the Laughlin quasiparticles.
- ²²D. V. Averin and A. N. Korotkov, Sov. Phys. JETP **70**, 937 (1990).
- ²³A. T. Johnson, L. P. Kouwenhoven, W. de Jong, N. C. van der Vaart, C. J. P. M. Harmans, and C. T. Foxon, Phys. Rev. Lett. **69**, 1592 (1992).
- ²⁴In Ref. 9 Nagaosa and the present author incorrectly predicted a slightly different line shape, though they obtained the correct temperature dependence of the peak conductance, which was the main issue in Ref. 9. This error is made because $T\gamma(0,T)$ is used as a level width of an intermediate state in Ref. 9. If we replace Γ in Eq. (11) of Ref. 9 with $T\cosh(\varepsilon/2T)\gamma(\varepsilon,T)$, we get the correct result, Eq. (19) of the present paper. The calculation in Ref. 9 corresponds to taking T as a low-energy cutoff for the renormalization even when $\varepsilon > T$. Note that $T\cosh(\varepsilon/2T)\gamma(\varepsilon,T) \propto (\max\{2\pi T, \varepsilon\})^{1/g-1}$.
- ²⁵D. V. Averin and Yu. V. Nazarov, Phys. Rev. Lett. **65**, 2446 (1990).
- ²⁶T. K. Ng and P. A. Lee, Phys. Rev. Lett. **61**, 1768 (1988).
- ²⁷L. I. Glazman and M. E. Raikh, JETP Lett. **47**, 452 (1988).
- ²⁸K. A. Matveev, Sov. Phys. JETP **72**, 892 (1991).
- ²⁹K. Moon, H. Yi, C. L. Kane, S. M. Girvin, and M. P. A. Fisher, Phys. Rev. Lett. **71**, 4381 (1993).
- ³⁰P. Fendley, A. W. W. Ludwig, and H. Saleur, Phys. Rev. Lett. **75**, 2196 (1995).
- ³¹The universal line shape was derived in Ref. 14 by integrating out a massive mode to reduce a double-barrier system to a single-barrier problem. This procedure is justified only in the limit of weak backscattering.